

Structure, Substructure, Hardness and Adhesion Strength of Multiperiod Composite Coatings MoN / CrN

S.S. Grankin¹, V.M. Beresnev¹, O.V. Sobol², V.A. Stolbovoy³, V.Yu. Novikov⁴, S.V. Lytovchenko¹,
U.S. Nyemchenko¹, A.A. Meylehov², M.G. Kovaleva⁴, A.A. Postelnik², I.N. Toryanik¹

¹ V.N. Karazin Kharkiv National University, 4, Svobody Sq., 61022 Kharkiv, Ukraine

² National Technical University "Kharkiv Polytechnic Institute", 21, Frunze Str., 61002 Kharkiv, Ukraine

³ National Science Center "Kharkiv Institute of Physics and Technology",
1, Akademicheskaya St., 61108 Kharkiv, Ukraine

⁴ Belgorod National Research University, 85, Pobedy St., 308015 Belgorod, Russia

⁵ Scientific Center of Physical Technologies of MES and NAS of Ukraine, 6, Svobody Sq., 61022 Kharkiv, Ukraine

(Received 09 November 2015; published online 10 December 2015)

A comprehensive study of the influence of the thickness of the layers, U_s and P_N on the structural engineering to obtain high mechanical properties in multilayer composite MoN / CrN vacuum-arc coatings has been conducted by means of scanning electron microscopy with energy analysis, X-ray diffraction studies microindentation and scratch testing methods. It has been determined that in the studied $P_N = (2-30) \times 10^{-4}$ Torr, the content of nitrogen in the coatings varies from 6.3 to 33 at. %, which leads even at the greatest nitrogen content to the formation of lower phase by nitrogen, γ -Mo₂N and isostructural CrN with the vacant sites in the nitrogen sublattice. The increase of thickness of the layers applied on the substrate in a stationary state promotes the increase of nitrogen content. Along with this, the lowest microdeformation and the average size of crystallites are formed at $U_b = -300$ V, which defines the achievement of greater hardness of 35 GPa and high adhesion strength, which resists the destruction, $L_{c5} = 187.6$ N.

Keywords: Vacuum-arc coatings, Multilayer coating, Hard coatings, Vacuum-arc deposition.

PACS numbers: 61.46. – w, 62.20.Qp, 62.65. – g

1. INTRODUCTION

Analysis of the development of modern technologies shows the urgent need in establishment of the universal materials in their functional properties, which is largely achieved by varying the phase-structural states of the surface layers (surface engineering) [1-6]. Compounds of metals with nitrogen (nitrides) are of particular interest, because of high chemical resistance in various aggressive environments, which is inherent to a set of phases, and refractoriness, high hardness, dielectric and semiconductor properties, etc. [7-15]. Since the natural materials have quite limited capacities, the intensive development in recent years has been after creating new artificial materials, and one of the most promising methods is creating multi-periodic structures [16-20]. In these methods by means of combination of layers with different elemental composition and phase-structural states, the universal functions of material by functional properties is achieved [21-23].

Multilayer coatings based on MoN / CrN are among the most perspective systems of vacuum-arc multilayer coatings. In this system, the layers of Mo-N provide the combination of high hardness with high heat resistance with a relatively small thermal expansion coefficient, and layers of Cr-N provide high corrosion resistance, wear resistance and resistance to degradation at elevated temperatures.

The aim of this study was to conduct the necessary for structural engineering analysis of the relationship of the phase composition, structure, substructure characteristics changed by varying the pressure of the working atmosphere, the thickness of layers and negative bias potential applied to the substrate, and func-

tional mechanical properties (hardness and adhesion strength) of composite multilayer MoN / CrN vacuum-arc coatings.

2. SAMPLES AND RESEARCH METHODS

The samples were obtained by means of vacuum-arc deposition method on a modernized "Bulat-6" installation [24]. The pressure of working atmosphere (nitrogen) during the deposition was $P_N = (2-30) \times 10^{-4}$ Torr. The deposition was carried out from two sources (Mo and Cr) at continuous rotation of the samples fixed on the substrates with a speed of 8 rev/min, which made it possible to obtain a layer with a thickness of about 7 nm, with the total number of layers of 960 (or 480 bilayer periods), and by means of fixing the substrate close to the targets with the duration of deposition of layers of 10, 20, 40, 150 and 300 seconds and the total thickness of the coating at all the used modes of about 10 microns. During the deposition a constant negative potential $U_b = -20, -40, -150, -300$ V was applied to the substrate.

Phase and structural analysis was carried out by X-ray diffraction method in Cu-K α emission. The separation of the profiles by their components was carried out using the software package «New Profile».

The hardness was measured by means of microindentation method, with Vickers diamond pyramid as an indenter at loads of 25, 50 and 100 g. The study was carried out on the device for testing microhardness 402MVD by Instron Wolpert Wilson Instruments.

Investigation of the coatings for determining adhesive and cohesive strength, resistance to scraping and finding out a mechanism of destruction was carried out

with Revetest scratch-tester (CSM Instruments). Scratches were made on the surface of the coating with a help of "Rockwell C" spherical indenter with a rounding radius of 200 μm at continuously increasing load. At the same time the power of acoustic emission, friction coefficient and penetrating depth, as well as the magnitude of normal load have been measured. To obtain reliable results, three scratches were applied over the surface of each coated sample. The tests were performed under the following conditions: the load over the indenter was increasing from 0.9 to 70 N, the sliding speed was 1 mm/min, the length of a scratch – 10 mm, loading speed – 6.91 N/min, the frequency of discreteness of a signal 60 Hz, acoustic emission signal power – 9 Db.

3. RESULTS AND DISCUSSION

As seen from the side cut area, a multi-layer coating (Fig. 1) differs with a sufficiently high planarity of layers and the absence of drop phase in the interior areas of the coating.

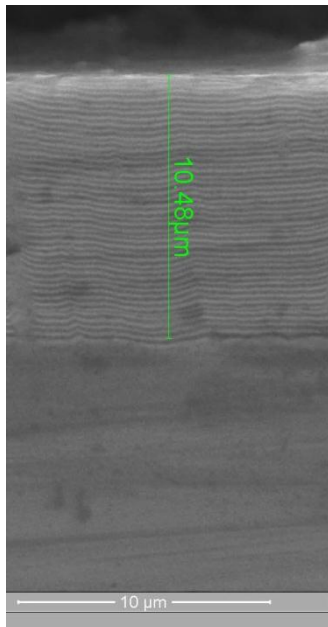
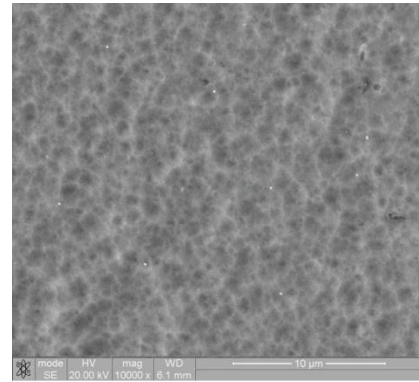
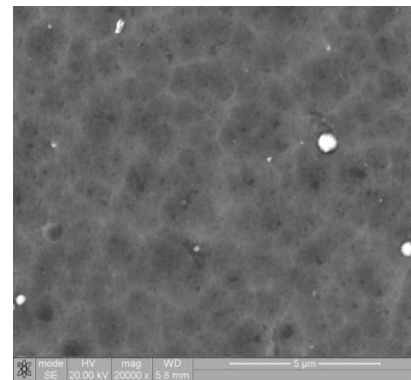


Fig. 1 – The image of multilayer coating

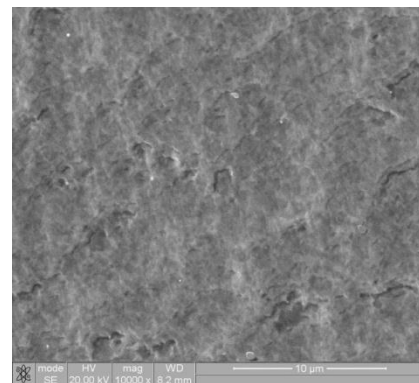
The surface of the coatings is much more heterogeneous, especially for the coatings obtained at a relatively low pressure $P_N = (2.7) \times 10^{-4}$ Torr. Also, at a large U_b , the difference in the surface morphology of the coatings is observed with different numbers of layers. As seen from the photographs of the surface of the coatings obtained at $U_b = -300$ V at different thickness and number of layers, at the lowest thickness of the layers (continuous rotation) of about 5-7 nm, the surface consists of small erosion pits with an average size of less than 1 micron (see Fig. 2a). With increasing the thickness of layers to 200 nm, an average size of erosion pits is increased to 1.5-1.7 μm (see Fig. 2b), while at lowering the pressure to $P_N = 2.7 \times 10^{-4}$ Torr there is a significant amount of droplet phase on the surface with a size of 1 to 3 microns (see Fig. 2).



a



b



c

Fig. 2 – The surface morphology of the multilayer coatings obtained at a pressure $P_N = 3 \times 10^{-3}$ Torr with the average thickness of layers of 6 nm (a) and 200 nm (b), and at $P_N = 2.7 \times 10^{-4}$ Torr (c)

Energy-dispersive spectra of the coatings MoN/CrN obtained at $U_b = -300$ V and pressure $P = 3 \times 10^{-3}$ Torr with different layer thicknesses, as well as at a low pressure of 7×10^{-4} Torr indicate, which shows that with the that the increase of thickness from 50 to 100 nm, the change in the atomic ratio of Mo/Cr atoms upward chromium occurs. At the same time, lowering the pressure of the working atmosphere to 7×10^{-4} Torr causes a sharp decrease of the peak corresponding to nitrogen.

The results of elemental analysis show that for small thicknesses, when the layers are the thinnest and the most significant portion of time during precipitation have goes for high speed rotation of the surface

and interaction with residual gases in the working chamber; the depletion of the layers of the coating with light nitrogen atoms (Fig. 3) occurs.

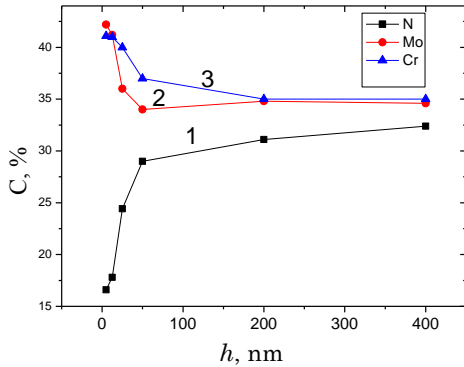


Fig. 3 – Dependence of the content of atoms of nitrogen (1), molybdenum (2), and chromium (3) on the thickness of the layers of the multilayer composite material MoN / CrN

It should be noted that at thicknesses greater than 50 nm, the content of elements in the coating comes to values close to constant, and at a pressure of 3×10^{-3} Torr makes a proportion close to 1 between the metal atoms, and about 33 % of nitrogen, which corresponds to the stoichiometry of the phases Me_2N (where Me are metal atoms: Mo or Cr). At a lesser pressure of 7×10^{-4} Torr and 2.4×10^{-4} Torr, the nitrogen contents drops sharply to 17.09 and 6.33 at. %, respectively.

Analysis of diffraction spectra of the coatings shows that in the case of a small value of the negative bias potential applied to the substrate during the deposition (-20 V) in the spectra (Fig. 4) for all the layer thicknesses in the range of 5-200 nm, phases with cubic lattices based on fcc with a weak texture with the axis [311], typical for given regimes in monolayer state for γ - Mo_2N phase [25].

Increasing the bias potential to -150 V and -300 V leads to formation of texture with [100] axis in the layers and to increase in its intensity with increasing the thickness of the layer.

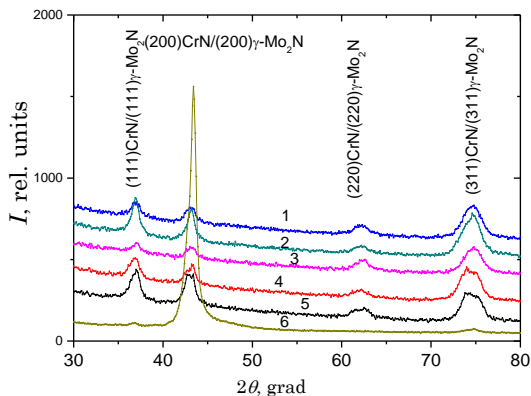


Fig. 4 – Areas of diffraction spectra of the coatings obtained at $P_N = 3 \times 10^{-3}$ Torr and $U_b = -20$ V at thickness of the layers of: 1 – 6 nm, 2 – 13 nm, 3 – 25 nm, 4 – 50 nm, 5 – 200 nm and $U_b = -300$ V at thickness of the layers of 13 nm (6)

On a substructural level at the lowest $U_b = -20$ V with the increase of thickness of the layer, the growth of the average crystallite size and nonmonotonic mi-

crostrain behavior are observed: from high values (1.5 %) with a layer thickness of less than 20 nm, through a minimum (1.1 %) at $h \approx 100$ nm to 1.4 % at large thicknesses (see Fig. 5a).

With an increase of U_b up to -150 V in the absolute magnitude, a decrease in microstrain in the layers both by absolute value (0.8-1.05 %), and by amplitude takes place.

The average crystallite size varied non-monotonically – increasing proportionally to the thickness of the layer to a thickness of 100 nm, and then reduced by 40 % with a further increase of the layer thickness.

For highest $U_b = -300$ V used in paper, the value of microstrain in the layers did not exceed 0.4 % (see Fig. 6b), and the crystallite size was also the smallest of the considered for the respective thicknesses. The observed decrease in microdeformation tells of recombination processes, stimulated by higher density of radiation defects along with the increase of the mean energy of the film-forming particles as a result of increase of U. The decrease of the average size of crystallites can be linked with the intense action of the defects, which increases the growth of centers of formation.

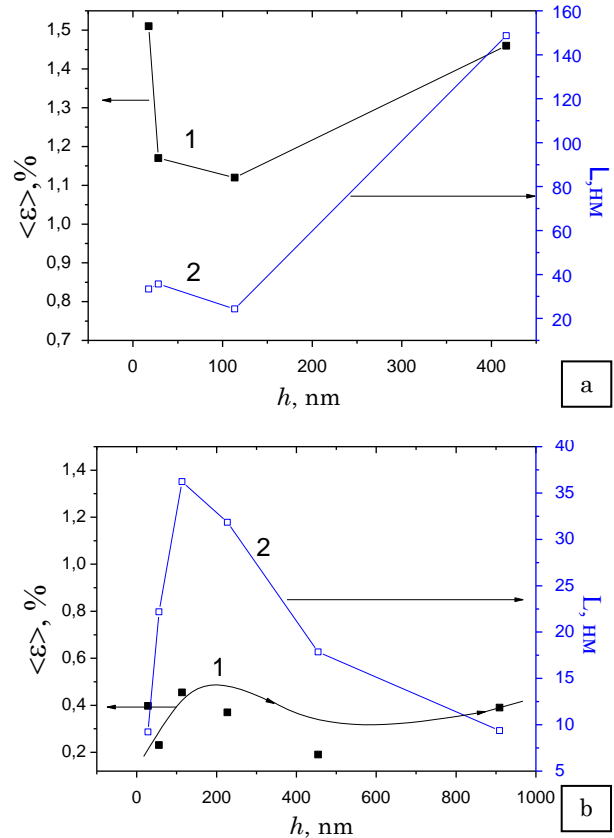


Fig. 5 – Dependence of substructural characteristics (microdeformation $\langle \epsilon \rangle$ (1) and the size of crystallites L (2)) on the thickness of the layers in the coatings obtained at $U_b = -20$ V (a) and $U_b = -300$ V (b)

The smaller size of the crystallites and hence a larger average specific volume of the borders defines a higher relaxation capacity for the randomly formed dislocation defects, which define microstrain.

The presence of a small microdeformation and grain size of crystallites may be factors of increasing the

adhesive strength of the material. Thus, for adhesive strength tests, the coatings obtained at $U_b = -300$ V with different layer thicknesses have been chosen.

The conducted studies have shown that for the entire range of the used thicknesses of the layers, the uniform wear of the coating over the entire range of applied loads takes place in the composite coatings; this is manifested in the homogeneity of acoustic emission spectrum (see Fig. 6, spectrum 1). Along with this, the coefficient of friction for all the thicknesses of the coatings is sufficiently close and is in the range of 0.18-0.24 (see Fig. 6, spectrum 2)

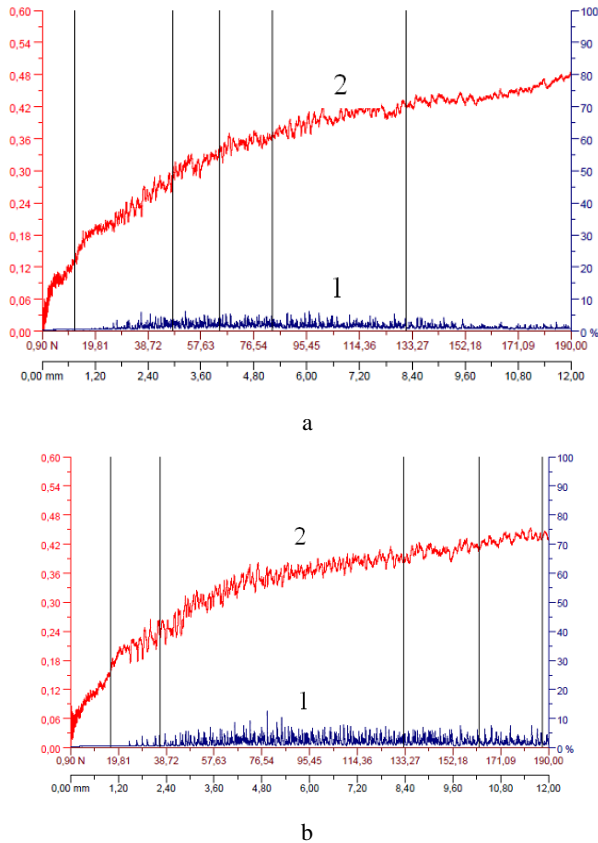
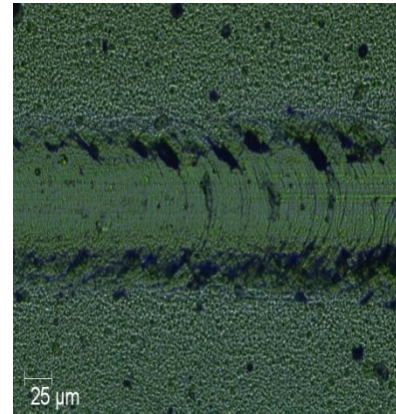


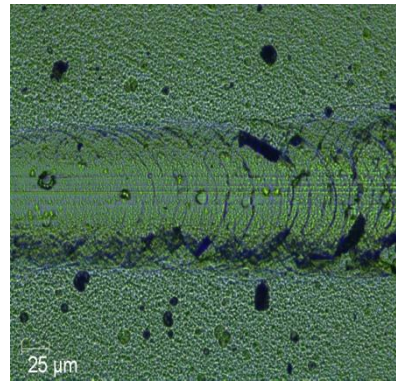
Fig. 6 – Change in the average values of the amplitude of the acoustic emission (spectrum 1, right scale) and the coefficient of friction (spectrum 2, left scale) for the coatings produced at $P_N = 3.10^{-3}$ Torr and $U_b = -300$ V at the thickness of the layers: a – 13 nm, b – 400 nm

Along with this, the nature of wear with the decrease of the thickness of the layers becomes more uniform, which is especially evident at the areas of the first critical load L_{C1} (see Fig. 7). This indicates a decrease in brittleness (ductility increase) of the layers along with decreasing h . Such changes may be related to a decrease of the average crystallite size and microstrain in this case (see Fig. 6b). In this case, the critical load value is determined by a decisive role of coating hardness value, which with the increase of thickness of the layers varied from 23 to 35 GPa.

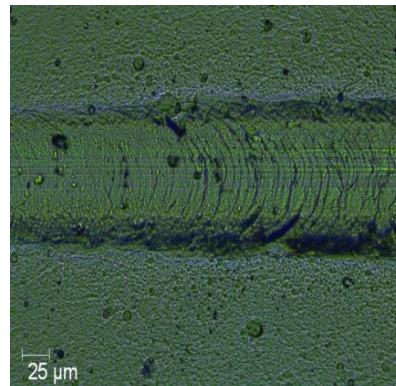
Along with this, the most ductile form of wear (see Fig. 9) is characteristic for the coatings obtained at low



a



b



c

Fig. 7 – Wear tracks at critical loads L_{C1} for the coatings produced at $P_N = 3 \times 10^{-3}$ Torr and $U_b = -300$ V at the following layer thicknesses: a – 400 nm, b – 200 nm, c – 13 nm

pressure and reducing the nitrogen content, which determines strong covalent interatomic bonds. The hardness of these coatings is 4-7 GPa.

Summary data on the critical load abrasion of the coatings L_{C5} shown in Table 1 for the coatings produced at $P_N = 3 \times 10^{-3}$ Torr and $U_b = -300$ V show that the adhesion strength is great for all layer thicknesses of such coatings, however, the increase in the thickness and hardening allows reaching the maximum value $L_{C5} = 185-187$ N at the thicknesses of the layers of 200-400 nm.

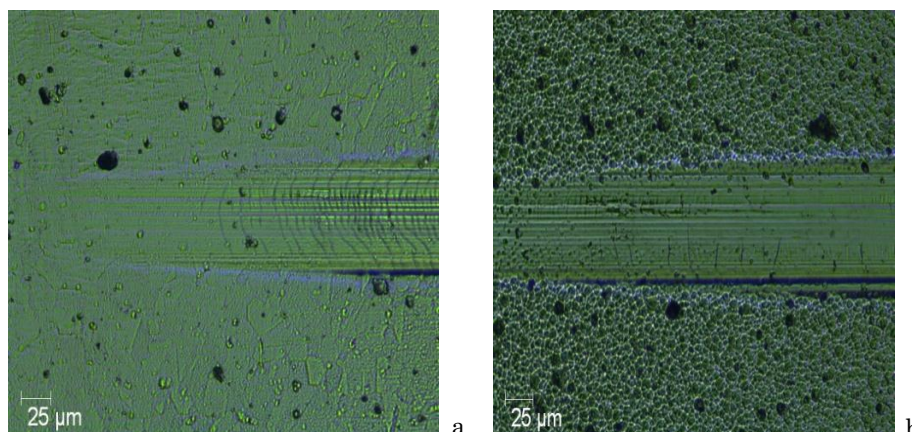


Fig. 8 – Wear tracks at critical loads L_{C1} for the coatings produced at $P_N = 7 \times 10^{-4}$ Torr (a) and $P_N = 2 \times 10^{-4}$ Torr (b)

Table 1 – Critical load L_{C5} for the coatings obtained at $P_N = 3 \times 10^{-3}$ Torr, $U_b = -300$ V and different thickness of layers

The thickness of layers, h , nm	L_{C5} , N
13	130.9
25	152.1
50	156.7
100	157.3
200	185.7
400	187.6

It should be noted that for the initial stage of wear, the critical load for the coatings produced at $P_N = 3 \times 10^{-3}$ Torr is in the range of 13-18 N, whereas for the plastic coatings, obtained at low pressure of nitrogen atmosphere, the value L_{C1} is much lower, and has values of 6 and 4 N, respectively, for $P_N = 7 \times 10^{-4}$ Torr and $P_N = 2 \times 10^{-4}$ Torr.

REFERENCES

1. *Nanostructured Coatings* (Ed by Albano Cavaleiro, Jeff Th. M. De Hosson) (Springer-Verlag: 2006).
2. P.H. Mayrhofer, C. Mitterer, L. Hultman, H. Clemens, *Prog. Mater. Sci.* **51**, 1032 (2006).
3. O.V. Sobol', *Phys. Solid State* **53** No 7, 1464 (2011).
4. C. Mitterer, P.H. Mayrhofer, J. Musil, *Vacuum* **71**, 279 (2005).
5. O.V. Sobol', O.N. Grigorjev, Yu.A. Kunitsky, S.N. Dub, A.A. Podtezhnikov, A.N. Stetsenko *Sci. Sintering* **38**, 63 (2006).
6. A.D. Pogrebnyak, V.N. Borysyuk, A.A. Baghdasaryan, O.V. Maksakova, E.V. Smirnova, *J. Nano- Electron. Phys.* **6** No 4, 04018 (2014).
7. S. Veprek, G.L. Maritz, et al., *Thin Solid Films* **476**, 1 (2005).
8. Musil, *Nanocomposite Thin Films and Coatings: Processing, Properties and Performance, Ch. 5* (Eds. by S. Zhang, A. Nasar) (London: Imperial College Press: 2007).
9. O.V. Sobol', A.A. Andreev, S.N. Grigoriev, V.F. Gorban', M.A. Volosova, S.V. Aleshin, V.A. Stolbovoy, *Metal Sci. Heat Treatm.* **54** No 3-4, 195 (2012).
10. N.A. Azarenkov, O.V. Sobol', V.M. Beresnev, A.D. Pogrebnyak, D.A. Kolesnikov, P.V. Turbin, I.N. Toryanik, *Metallofiz. Nov. Tekhnol.* **35** No 8, 1061 (2013).
11. V.M. Beresnev, O.V. Sobol', A.D. Pogrebnyak, P.V. Turbin, S.V. Litovchenko, *Techn. Phys.* **55** No 6, 871 (2010).
12. A. Horling, L. Hultman, M. Oden, J. Sjolen, L. Karlsson, *Surf. Coat. Technol.* **191**, 384 (2005).
13. R. Krause-Rehberg, A.D. Pogrebnyak, V.N. Borysyuk, M.V. Kaverin, A.G. Ponomarev, M.A. Bilokur, K. Oyoshi, Y. Takeda, V.M. Beresnev, O.V. Sobol', *Phys. Metal. Metallography.* **114** No 8, 672 (2013).
14. F.R. Lamastra, F. Leonardi, R. Montanari, F. Casadei, T. Valente, G. Gusmano, *Surf. Coat. Technol.* **200**, No 22-23, 6172 (2006).
15. A. Lousa, J. Romero, E. Martinez, J. Esteve, F. Montala, L. Carreras, *Surf. Coat. Technol.* **146-147**, 268 (2001).
16. Ch.K. Tien, J.-G. Duh, J.-W. Lee, *Surf. Coat. Technol.* **201**, 5138 (2007).
17. H.C. Barshilia, K.S. Rajam, *Surf. Coat. Technol.* **183**, 174 (2004).
18. M.A. Ertas, A.C. Onel, G. Ekinici, B. Toydemir, S. Durdu, M. Usta M., L. Colakerol, *Int. J. Chem., Nuclear, Mater. Metallurgical Eng.* **9** No 1, 53 (2015).
19. L. Chen, S.Q. Wang, S.Z. Zhou, J. Li, Y.Z. Zhang, *Int. J. Refractory Metal. Hard Mater.* **26**, 456 (2008).
20. M.S. Konchady, S. Yarmolenko, D.M. Pai, J. Sankar, *Proc. Eng. Appl. Novel Mater.* **14**, 55 (2009).
21. J.A. Alegria-Ortega, L.M. Ocampo-Carmona, F.A. Suárez-Bustamante, J.J. Olaya-Flórez, *Wear* **290-291**, 149 (2012).
22. R. Bayon, A. Igartua, X. Fernández, R. Martínez, R.J. Rodríguez, J.A. García J.A., A. de Frutos, M.A. Arenas, J. de Damborenea, *Tribology Int.* **42** No 4, 591 (2009).
23. A. Gilewicz, B. Warcholinski, *Tribology Int.* **80**, 34 (2014).
24. A.A. Andreev, L.P. Sablev, S.N. Grigoriev, *Vacuum- arc coatings*. (Kharkov: NSC KIPT: 2010).
25. O.V. Sobol', A.A. Andreev, V.A. Stolbovoy, V.F. Fil'chikov, *Techn. Phys. Lett.* **38** No 2, 168 (2012).